FINAL TECHNICAL REPORT

for

NASA/MSFC NAG8-1787 (5-21241)

University of Alabama in Huntsville
Department of Electrical and Computer Engineering
301 Sparkman Drive, Huntsville, Alabama 35899

IMPROVED RE-CONFIGURABLE SLIDING MODE CONTROLLER FOR REUSABLE LAUNCH VEHICLE OF SECOND GENERATION ADDRESSING AERODYNAMIC SURFACE FAILURES AND THRUST DEFICIENCIES

Principal Investigator: Dr. Yuri B. Shtessel, Professor
Electrical and Computer Engineering Department
University of Alabama in Huntsville, Huntsville, AL 35899
(256) 824-6164 (voice), (256) 824-6803 (fax)
email: shtessel@ece.uah.edu

Huntsville, 2002

ABSTRACT

In this report we present a time-varying sliding mode control (TV-SMC) technique for reusable launch vehicle (RLV) attitude control in ascent and entry flight phases. In ascent flight the guidance commands Euler roll, pitch and yaw angles, and in entry flight it commands the aerodynamic angles of bank, attack and sideslip. The controller employs a body rate inner loop and the attitude outer loop, which are separated in time-scale by the singular perturbation principle. The novelty of the TVSMC is that both the sliding surface and the boundary layer dynamics can be varied in real time using the PD-eigenvalue assignment technique. This salient feature is used to cope with control command saturation and integrator windup in the presence of severe disturbance or control effector failure, which enhances the robustness and fault tolerance of the controller. The TV-SMC is developed and tuned up for the X-33 sub-orbital technology demonstration vehicle in launch and re-entry modes. A variety of nominal, dispersion and failure scenarios have tested via high fidelity 6DOF simulations using MAVERIC/SIM simulation software.

1. INTRODUCTION

Flight control of both current and future reusable launch vehicles (RLV) in ascent and descent modes involves attitude maneuvering through a wide range of flight conditions, wind disturbances, and plant uncertainties including aerodynamic surfaces and engine failures. The baseline RLV flight control system that was designed for the X-33 technology demonstration sub-orbital launch vehicle employs a variable structure PID control law[1] with gain scheduling. This requires four gains per channel that are looked up from a table as a function of relative velocity. Depending on the flight trajectory, each gain table can have as many as 25 values, so potentially 300 gain values must be stored in the on board computer for nominal flight. In case of an engine failure, or Power Pack Out (PPO) alternate sets of gain tables are used, depending on the flight time when the failure occurred. Provisions are made for 25 possible PPO times, or 25 sets of PID tables. This amounts to another 7500 values to be stored, or a total of 7800 values to provide gains for the nominal and engine failed cases. The reason for so many gain tables is because the control system design relies on linear analysis and perturbation theory at specific design points along the trajectory. This method is well established and has been used in many launch vehicle control system designs. Robust control is

PROJECT OBJECTIVES

The proposed research is dedicated to improving sliding mode controller for reusable launch vehicles (RLV) of second generation to address aerodynamic surface failures and thrust deficiencies. The proposed research effort is an extension of the research done under the project titled "Advanced Guidance and Control for the RLV of Second Generation." This proposal contributes to risk reduction area associated with reduced controllability of RLV in presence of control effector failure and RLV model uncertainties. Availability of this type of control system would improve safety of the RLV, reduce operation cost for the RLV by reducing the pre-flight effort for each flight significantly. Increasing reliability/life of the entire system will be also achieved.

Flight control of the RLV of second generation involves large attitude maneuvers through a wide range of flight conditions from lift-off to entry. Improving recovery of tracking performance of the RLV from the aerodynamic surface failures and thrust deficiencies is achieved via re-configurable/adaptive time varying multiple loop continuous sliding mode controller (TV-SMC) design with a direct adaptation taking into account the torque command limitations. Providing a tracking performance recovery, the re-configurable adaptive time-varying continuous sliding mode controller will achieve robust, high-accuracy tracking of guidance trajectories for large attitude maneuvers through a wide range of flight conditions in presence of aerodynamic surface failures and thrust deficiencies and model uncertainties. The designed controller also will automatically adjust to changing specifications, such as mass of payload and target orbit, and the operating environment, such as atmospheric perturbations and interconnection perturbations from the other subsystems of the RLV. The TV-SMC will be developed and tuned up for the X-33 sub-orbital technology demonstration vehicle in launch and re-entry modes via high fidelity 6DOF simulations using MAVERIC/SLIM simulation software. A variety of failure scenarios will be tested.

ensured as long as the vehicle performance and operating conditions are relatively close to the design points. A robust flight control algorithm that would accommodate different trajectories and aerodynamic surface and engine failures without gain scheduling would be an improvement over the RLV current flight control technology. Sliding Mode Controller (SMC) is an attractive robust control algorithm for the RLV ascent and descent flight controller designs because of its inherent insensitivity and robustness to plant uncertainties and external disturbances[2-4]. Such a robust controller[5,6] would reduce risk and drastically decrease the amount of time spent in pre-flight analysis, thus reducing cost.

In this work we present a time-varying sliding mode controller (TV-SMC) design technique. The RLV fixed-gain (FG) SMC two-loop structure, which is developed in the works[5,6], is employed in this work for the TV-SMC design.

In the outer loop, the kinematics equation of angular motion is used with the outer loop SMC to generate the angular rate profiles as virtual control inputs to the inner loop. In the inner loop, a suitable inner loop SMC is designed so that the commanded angular rate profiles are tracked. The inner loop SMC produces roll, pitch and yaw torque commands, which are allocated into end-effector deflection commands. Multiple time scaling (multiple-scale) is defined as the time-constant separation between the two loops. That is, the inner loop compensated dynamics is designed to be faster than the outer loop dynamics. The resulting multiple-scale two-loop SMC, with optimal torque allocation, causes the angular rate and the Euler angle tracking errors to be constrained to linear de-coupled homogeneous vector valued differential equations with desired eigenvalues.

In this paper the TV-SMC design technique is presented for the attitude controller (autopilot) for RLV. Any partial or complete failure of control actuators and effectors will be inferred from saturation of one or more commanded control signals generated by the controller. The saturation causes a reduction in the effective gain, or bandwidth of the feedback loop. The controller cannot tell nor does it care whether control command saturation is due to wind gust or a stuck effector, because it only computes the required torque to eliminate the tracking error. A truly adaptive controller should be able to do this even if the vehicle has lost significant control authority due to control effector failure. It is up to the combination of the control allocation and the control effectors to realize the required torque. In order to maintain stability, the bandwidth of the nominal (reduced-order) system will be reduced accordingly using a time-varying bandwidth PD-eigenstructure

assignment technique[7,8]. The presented TV-SMC fault-tolerant technique automatically handles momentary saturations and integrator windup caused by excessive disturbances, guidance command or dispersions under normal vehicle conditions.

2. RLV ATTITUDE CONTROL PROBLEM

The rigid body equations of motion for an RLV is given by (1)-(5)

$$(\mathbf{J}_0 + \Delta\mathbf{J})\dot{\omega} = -\Omega(\mathbf{J}_0 + \Delta\mathbf{J})\omega + (\mathbf{I} + \mathbf{E})\mathbf{T} + \mathbf{d} \tag{1}$$

$$\dot{\gamma} = \mathbf{R}(\gamma)\omega \tag{2}$$

$$\Omega = \begin{bmatrix} 0 & -\omega_3 & \omega_2 \\ \omega_3 & 0 & -\omega_1 \\ -\omega_2 & \omega_1 & 0 \end{bmatrix} \tag{3}$$

where the rotational matrix $R(\gamma)$ for ascent is given by

$$\mathbf{R}(\gamma) = \begin{bmatrix} 1 & \tan\theta\sin\varphi & \tan\theta\cos\varphi \\ 0 & \cos\varphi & -\sin\varphi \\ 0 & \dfrac{\sin\varphi}{\cos\theta} & \dfrac{\cos\varphi}{\cos\theta} \end{bmatrix}, \quad \gamma = [\varphi \quad \theta \quad \psi]^T, \tag{4}$$

and the $R(\gamma)$ for entry

$$\mathbf{R}(\gamma) = \begin{bmatrix} \cos\alpha & 0 & \sin\alpha \\ 0 & 1 & 0 \\ \sin\alpha & 0 & -\cos\alpha \end{bmatrix}, \quad \gamma = [\varphi_b \quad \alpha \quad \beta]^T. \tag{5}$$

The control problem for the RLV in ascent and descent modes is to determine the control torque command vector $\mathbf{T}$ such that the commanded orientation angle profiles γ_c are robustly asymptotically followed in the presence of bounded disturbance torque $\mathbf{d}$, the RLV inertia variations $\Delta\mathbf{J}$ and aerodynamic surface and engine failures that are described by the uncertain matrix $\Delta\mathbf{D}(.)$, $\mathbf{E} = \Delta\mathbf{D}(.)\mathbf{D}^{\#}$, $\mathbf{D}^{\#}(.) = \mathbf{D}(.)^{\mathrm{T}}\left[\mathbf{D}(.)\mathbf{D}(.)^{\mathrm{T}}\right]^{-1}$, $\mathbf{D}(.)$ is a nominal sensitivity matrix.

3. SUMMARY OF THE SMOOTH MULTIPLE-LOOP FIXED-GAIN SLIDING MODE CONTROL

The smooth multiple-loop fixed-gain sliding mode controller is designed as follows[5,6]:

- The outer loop smooth fixed-gain SMC generates body rate commands

$$\omega_c = \mathbf{R}^{-1}(\gamma)[\dot{\gamma}_c + \mathbf{K}_1\gamma_e] + \mathbf{R}^{-1}(\gamma)\mathbf{K}_2\sigma \tag{6}$$

$$\sigma = \gamma_e + \mathbf{K}_1\int_0^t \gamma_e d\tau\,,\ \sigma \in \mathbf{R}^3,\ \gamma_e = \gamma_c - \gamma \tag{7}$$

or

$$\omega_c = \mathbf{R}^{-1}(\gamma)\left[\dot{\gamma}_c + (\mathbf{K}_1 + \mathbf{K}_2)\gamma_e + \mathbf{K}_2\mathbf{K}_1\int_0^t \gamma_e d\tau\right] \tag{8}$$

that provide the following outer loop compensated dynamics (given the ω_c profile is tracked perfectly in the inner loop):

$$\ddot{\gamma}_e + (\mathbf{K}_1 + \mathbf{K}_2)\dot{\gamma}_e + (\mathbf{K}_2\mathbf{K}_1)\gamma_e = 0\,. \tag{9}$$

- The inner loop smooth fixed-gain SMC generates control torque commands

$$\mathbf{T} = \mathbf{J}_0\dot{\omega}_c + \mathbf{J}_0\mathbf{K}_3\omega_e + \Omega\mathbf{J}_0\omega + \mathbf{J}_0\mathbf{K}_4 s \tag{10}$$

$$s = \omega_e + \mathbf{K}_3\int_0^t \omega_e d\tau\,,\quad s \in \mathbf{R}^3,\ \omega_e = \omega_{\cdot} - \omega \tag{11}$$

or

$$\mathbf{T} = \mathbf{J}_0\dot{\omega}_c + \Omega\mathbf{J}_0\omega_c + (\mathbf{J}_0\mathbf{K}_3 - \Omega\mathbf{J}_0 + \mathbf{J}_0\mathbf{K}_4)\omega_e + \mathbf{J}_0\mathbf{K}_4\mathbf{K}_3\int_0^t \omega_e d\tau \tag{12}$$

that provide the following inner loop compensated dynamics (given the $\mathbf{T}$ profile is allocated perfectly into commands to actuator deflections):

$$\dot{\omega}_e + (\mathbf{K}_3 + \mathbf{K}_4)\dot{\gamma}_e + (\mathbf{K}_4\mathbf{K}_3)\gamma_e = 0 \tag{13}$$

- Writing inner and outer loop tracking error equations in a damping factor/natural frequency format

$$\ddot{x} + 2\xi\omega_n\dot{x} + \omega_n^2 x = 0 \tag{14}$$

it is easy to calculate elements of diagonal matrices $\mathbf{K}_1, \mathbf{K}_2, \mathbf{K}_3$ and $\mathbf{K}_4$ to provide given damping factors (usually all are equal to 1.1 or so) and natural frequencies that provide for a sufficient time-scale separation between the control loops to eqs. (9) and (13) for inner and outer loop compensated tracking dynamics.

- Commands to the actuator deflections can be calculated as follows

$$\begin{cases} \delta_c = \delta_{c0} + \tilde{\delta}_c \\ \tilde{\delta}_c = \mathbf{D}(.)\mathbf{T}\Big|_{\mathbf{T}=\mathbf{J}_0\dot{\omega}_c+\Omega\mathbf{J}_0\omega_c+(\mathbf{J}_0\mathbf{K}_3-\Omega\mathbf{J}_0+\rho_2\mathbf{J}_0\mathbf{K}_4)\omega_e+\rho_2\mathbf{J}_0\mathbf{K}_4\mathbf{K}_3\int_0^t\omega_e d\tau} \end{cases} \tag{15}$$

where δ_{c0} is a bias command that should trim the RLV, $\mathbf{D}(.)$ is a sensitivity matrix (for a feedforward control allocation case).

4. SMOOTH MULTIPLE-LOOP TIME-VARYING SLIDING MODE CONTROL

Motivations. The elements of the command torque vector (12) are limited by physical abilities of the RLV flight control system that implies the following limits to elements of the vector $\mathbf{T}$:

$$a_i(.) \le T_i \le b_i(.), \qquad i = \overline{1,3}. \tag{16}$$

$$a_i'(.) \le \frac{d}{dt}T_i \le b_i'(.), \quad i = \overline{1,3} \tag{17}$$

where $a_i(.), b_i(.), a_i'(.), b_i'(.)$ depend on the RLV current flying conditions including Mach number, dynamic pressure and trim conditions. Designing the time-varying SMC inequalities (17) could be originally out of consideration.

The components of the vector $\mathbf{T}$ that depend on body rate tracking profile, ω_c, and its derivative, $\dot{\omega}_c$, usually have the largest amplitudes among the others. So, the following idea is proposed: if the inequalities (16) and/or (17) are about to be violated we have to start reducing magnitudes of the terms ω_c and $\dot{\omega}_c$ to prevent actuators from saturation. It will be achieved via real time adjusting bandwidths of inner and outer flight control loops. This procedure requires application of time-varying linear control technique[7,8] that is incorporated into the time-varying sliding mode controller design.

The following outer, ω_c, and inner, $\mathbf{T}$, continuous, time-varying sliding mode control (TV-SMC) laws are designed

$$\omega_c = \mathbf{R}^{-1}(\gamma)[\dot{\gamma}_c + \mathbf{K}_1(t)\gamma_e] + \mathbf{R}^{-1}(\gamma)\mathbf{K}_2(t)\sigma \tag{18}$$

$$\mathbf{T} = \mathbf{J}_0\dot{\omega}_c + \mathbf{J}_0\mathbf{K}_3(t)\omega_e + \Omega\mathbf{J}_0\omega + \mathbf{J}_0\mathbf{K}_4(t)s \tag{19}$$

where the outer, σ, and inner, s, sliding quantities are identified

$$\sigma = \gamma_e + \left(\mathbf{K}_1(t) - \mathbf{K}_2(t)^{-1}\dot{\mathbf{K}}_1(t)\right)\int_0^t \gamma_e d\tau, \ \sigma \in \mathbf{R}^3, \quad \gamma_e = \gamma_c - \gamma \tag{20}$$

$$s = \omega_e + \left(\mathbf{K}_3(t) - \mathbf{K}_4(t)^{-1}\dot{\mathbf{K}}_3(t)\right)\int_0^t \omega_e d\tau, s \in \mathbf{R}^3, \quad \omega_e = \omega_c - \omega \tag{21}$$

Remark. One can observe an apparent difference between the eqs. (20), (21) and eqs. (7), (11). These equations become identical if $\mathbf{K}_1 = const$ and $\mathbf{K}_3 = const$

The diagonal elements of the matrices $\mathbf{K}_2(t)$ and $\mathbf{K}_4(t)$ determines the time-varying thickness of the boundary layers of the outer and inner loops, respectively. Once $\mathbf{K}_2(t)$ and $\mathbf{K}_4(t)$ are fixed, $\mathbf{K}_1(t)$ and $\mathbf{K}_3(t)$ define the dynamics of the sliding modes of the outer and inner loops, respectively. When these controller gains are chosen in a certain manner as defined below, they can be used to define the desired time-varying bandwidths of the outer and inner loops. These bandwidths can be adjusted in real time to prevent actuators from saturation. The corresponding bandwidths or natural frequency of the compensated loop dynamics are to be decreased if the actuator command is close to saturation and are to be increased otherwise.

5. CONTROLLER DESIGN STABILITY ASSESSMENT: NOMINAL CASE

In the nominal case where $\mathbf{E} = \mathbf{0}, \quad \Delta\mathbf{J} = \mathbf{0}, \quad \mathbf{d} = \mathbf{0}$, the mathematical model of the RLV in eqs. (1)-(5) is completely known. For the outer loop, substituting eqs. (18) and (20) into eq. (2) and differentiating eq. (2) we obtained the compensated outer loop error dynamics

$$\dddot{\tilde{\gamma}}_e + (\mathbf{K}_1(t) + \mathbf{K}_2(t))\ddot{\tilde{\gamma}}_e + \left(\mathbf{K}_1(t)\mathbf{K}_2(t) - \dot{\mathbf{K}}_1(t)\right)\dot{\tilde{\gamma}}_e = \mathbf{R}\tilde{\omega}_e, \quad \tilde{\gamma}_e = \int_0^t \gamma_e(\tau)d\tau \tag{22}$$

Assume that the transient response in the inner, "faster", loop is stable and $\omega = \omega_c$ in eqs. (2) and (18). Then the tracking error $\tilde{\omega}_e$ is stabilized in the inner loop at zero. Assuming $\dot{\tilde{\omega}}_e = 0$ the equation (22) can be rewritten in a homogeneous format

$$\dddot{\tilde{\gamma}}_e + (\mathbf{K}_1(t) + \mathbf{K}_2(t))\ddot{\tilde{\gamma}}_e + \left(\mathbf{K}_1(t)\mathbf{K}_2(t) - \dot{\mathbf{K}}_1(t)\right)\dot{\tilde{\gamma}}_e = 0 \tag{23}$$

Since the matrices $\mathbf{K}_1(t)$ and $\mathbf{K}_2(t)$ are diagonal, eq. (23) can be rewritten in a scalar format

$$\dddot{\tilde{\gamma}}_{ei} + (k_{1i}(t) + k_{2i}(t))\ddot{\tilde{\gamma}}_{ei} + \left(k_{1i}(t)k_{2i}(t) - \dot{k}_{1i}(t)\right)\dot{\tilde{\gamma}}_{ei} = 0, \ \forall i = \overline{1,3} \tag{24}$$

The series D-eigenvalues of LTV differential equations (24) can be identified as follows

$$\lambda_{1i}(t) = -k_{1i}(t), \quad \lambda_{2i}(t) = -k_{2i}(t), \ \forall i = \overline{1,3}. \tag{25}$$

In order to assign values for the bandwidth (cut-off frequency or natural frequency) and damping factor for the compensated dynamics of the outer loop eqs. (24) are rewritten in a format

$$\ddot{\tilde{\gamma}}_{ei} + \left(2\xi_i \omega_{ni}(t) - \frac{\dot{\omega}_{ni}(t)}{\omega_{ni}(t)} \right) \dot{\tilde{\gamma}}_{ei} + \omega_{ni}^2(t) \tilde{\gamma}_{ei} = 0 \,,\ \xi_i > 1 \ \ \forall i = \overline{1,3} \,. \tag{26}$$

Then the so-called "PD-eigenvalue" can be identified as follows:

$$\Lambda_1(t) = \left(-\xi_i + \sqrt{\xi_i^2 - 1} \right) \omega_{ni}(t) \tag{27}$$

$$\Lambda_2(t) = \left(-\xi_i - \sqrt{\xi_i^2 - 1} \right) \omega_{ni}(t) \tag{28}$$

Note that for time-varying $\omega_{ni}(t)$, the relations between the sign of the radicals and the index of Λ_i must be maintained. Then the SD-eigenvalues are related to the PD-eigenvalues as follows

$$\lambda_{1i}(t) = \Lambda_1(t) = \left(-\xi_i + \sqrt{\xi_i^2 - 1} \right) \omega_{ni}(t) = -k_{1i}(t) \,, \forall i = \overline{1,3} \tag{29}$$

or

$$k_{1i}(t) = \left(\xi_i - \sqrt{\xi_i^2 - 1} \right) \omega_{ni}(t) \tag{30}$$

and

$$\lambda_{2i}(t) = \Lambda_{2i}(t) + \frac{\dot{\omega}_{ni}(t)}{\omega_{ni}(t)} = \left(-\xi_i - \sqrt{\xi_i^2 - 1} \right) \omega_{ni}(t) + \frac{\dot{\omega}_{ni}(t)}{\omega_{ni}(t)} = -k_{2i}(t) \tag{31}$$

or

$$k_{2i}(t) = \left(\xi_i + \sqrt{\xi_i^2 - 1} \right) \omega_{ni}(t) - \frac{\dot{\omega}_{ni}(t)}{\omega_{ni}(t)} \tag{32}$$

Thus, given ξ_i and $\omega_{ni}(t)$ the corresponding time-varying coefficients in the sliding surface (8) can be computed using eqs. (30) and (32).

Remarks.

1. The outer loop dynamics are obviously decoupled and the stability is guranteed by the PD-eigenvalues for $\xi_i > 1$ and $\omega_{ni}(t) > 0, \forall t \geq t_0$, which can be achieved by the choice of diagonal time-varying matrices $\mathbf{K}_1(t), \mathbf{K}_2(t)$ according to (30) and (32).

2. The gain matrices $\mathbf{K}_1(t), \mathbf{K}_2(t)$ must be selected in accrdance with (30) and (32) with $\xi_i > 1$ in order to to make σ - dynamics faster then $\tilde{\gamma}_e$-dynamics. The time scale separation increases with ξ_i. Note that (30) and (32) are for constant ξ_i only, and as such ξ_i should not be

adjusted in real time. The PD-eigenvalue synthesis formulas for time-varying $\xi_i(t)$ is available, but it is much more complex.

The inner loop compensated error dynamics are described by the eqs. (1), (3), (19) and (21), which can be combined as

$$\ddot{\tilde{\omega}}_e + (K_3(t) + K_4(t))\dot{\tilde{\omega}}_e + \left(K_3(t)K_4(t) - \dot{K}_3(t)\right)\tilde{\omega}_e = 0, \quad \tilde{\omega}_e = \int_0^t \omega_e(\tau)d\tau \tag{33}$$

Eq. (33) can be rewritten in a scalar "damping factor-natural frequency" format $\forall i = \overline{1,3}$

$$\ddot{\tilde{\omega}}_{ei} + \left(2\hat{\xi}_i\hat{\omega}_{\text{ni}}(t) - \frac{\dot{\hat{\omega}}_{\text{ni}}(t)}{\hat{\omega}_{\text{ni}}(t)}\right)\dot{\tilde{\omega}}_{ei} + \hat{\omega}_{\text{ni}}^2(t)\tilde{\omega}_{ei} = 0, \ \hat{\xi}_i > 1. \tag{34}$$

Eqs. (33) and (34) is a full anology to eqs. (24) and (26). So, the following coefficients can be identified by analogy

$$k_{3i}(t) = \left(\hat{\xi}_i - \sqrt{\hat{\xi}_i^{\,2} - 1}\right)\hat{\omega}_{\text{ni}}(t) \tag{35}$$

$$k_{4i}(t) = \left(\hat{\xi}_i + \sqrt{\hat{\xi}_i^{\,2} - 1}\right)\hat{\omega}_{\text{ni}}(t) - \frac{\dot{\omega}_{\text{ni}}(t)}{\omega_{\text{ni}}(t)} \tag{36}$$

Now, given $\hat{\xi}_i$ and $\hat{\omega}_{\text{ni}}(t)$ the corresponding time-varying coefficients in the sliding surface (21) can be computed concerning eqs. (18) and (19) $\forall i = \overline{1,3}$.

Remark. The same comments for $\mathbf{K}_1(t), \mathbf{K}_2(t)$ following (30) and (32) are applicable to $\mathbf{K}_3(t), \mathbf{K}_4(t)$ in relation to (35) and (36), and the s - dynamics and ω_e-dynamics.

6. STABILITY ASSESSMENT: PERTURBED CASE

In the perturbed case assume $\mathbf{E} \neq \mathbf{0}$, $\Delta\mathbf{J} \neq \mathbf{0}$, $\mathbf{d} \neq \mathbf{0}$, unknown but bounded, i.e. the math model of the RLV in eqs. (1)-(5) is not completely known. For the outer loop, again assume that the transient in the inner "faster" loop is stable and $\omega = \omega_c$ in eqs. (2) and (18). Then the perturbed case coinsides with the nominal case, since eqs. (2), (4) and (5) do not contain uncertaintes and disturbances.

The inner loop error compensated dynamics are described by the eqs. (1), (3), (19) and (21). In the perturbed case this is

$$\ddot{\tilde{\omega}}_e + (K_3(t) + K_4(t))\dot{\tilde{\omega}}_e + \left(K_3(t)K_4(t) - \dot{K}_3(t)\right)\tilde{\omega}_e = F(\tilde{\omega}_e, \dot{\tilde{\omega}}_e, \ddot{\tilde{\omega}}_e, t) \tag{37}$$

where $F(\omega_e, \dot{\omega}_e, \ddot{\omega}_e, t)$ depends on perturbation terms. The closed-loop stability of the perturbed system can be justified by the well-known results from the Lyapunov analysis[9].

Theorem. *Given a perturbed linear time-varying dynamic system*

$$\dot{x} = A(t)x + F(x,t) \tag{38}$$

where $\|F(x,t)\| \le \delta$ *is a bounded, nonvanishing perturbation, i.e.* $F(0,t) \neq 0$, *and the matrix* $A(t)$ *is Hurwitz, i.e. there exists a pair of positive definite matrices* $(P(t), Q(t))$ *satisfying the Lyapunov equation*

$$\dot{P}(t) + P(t)A(t) + A^T(t)P(t) = -Q(t) \tag{39}$$

such that

$$c_1\|x(t)\|^2 \le x^{\mathrm{T}}(t)P(t)x(t) \le c_2\|x(t)\|^2 \tag{40}$$

$$x^{\mathrm{T}}(t)Q(t)x(t) \le -c_3\|x(t)\|^2 \tag{41}$$

$$\|x^{\mathrm{T}}(t)P(t)\| \le c_4\|x(t)\| \tag{42}$$

for all $t > t_0$, *where* $\|v\| = \sqrt{v^{\mathrm{T}}v}$. *For any* $0 < \theta < 1$, *define*

$$\delta_0(\theta) = \frac{2c_3}{c_4}\sqrt{\frac{c_1}{c_2}}\theta \tag{43}$$

If $\|F(x,t)\| \le \delta < \delta_0$, *then every trajectory of the perturbed system is exponentially, ultimately bounded in the sense that for any* $r > 0$, *and* $\|x(t_0)\| \le r/k$, *there exists a* $t_1 > t_0$ *such that*

$$\|x(t,t_0)\| \le k\|x(t_0)\|\mathrm{e}^{-\lambda(t-t_0)}, \quad t_0 \le t < t_1, \tag{44}$$

$$\|x(t,t_0)\| \le b, \quad t \ge t_1, \tag{45}$$

where

$$k = \sqrt{\frac{c_2}{c_1}}, \ \lambda = \frac{(1-\theta)c_3}{2c_2}, \ b = \frac{\delta}{\delta_0(\theta)}r \tag{46}$$

7. SIMULATION

The results of following simulation tests performed on Slim 1.2 are presented:

1 Nominal flight evaluation.

2 Dispersion case evaluation.

3 Actuator-failed flight evaluation

Test1. Nominal Flight Evaluation

The goals and implementation conditions of the nominal flight evaluation test are

- Capability for generating control commands that assure RLV stability and high tracking accuracy is to be demonstrated.
- The aerodynamic model and actuator model is based on X-33 vehicle data.

Roll pitch and yaw angle tracking in *ascent* shown in Figures 1, 2 and 3 demonstrate high tracking accuracy.

The aerodynamic surface deflections that are shown in Figures 4 and 5 do not hit the limits.

Body torque ratios that are shown in Figure 6 demonstrate the fact that commanded torques are far from saturations, that's why the gain adaptation algorithm is not activated.

Angle of attack, bank angle and sideslip angle tracking in *descent* shown in Figures 7 - 9 demonstrate high tracking accuracy.

The aerodynamic surface deflections that are shown in Figures 10 and 11 do not hit the limits. The RCS propellant used in *descent* is shown in Figure 12.

The corresponding body torque ratios are far from limits, and the gain adaptation algorithm is not activated in *descent* nominal mode.

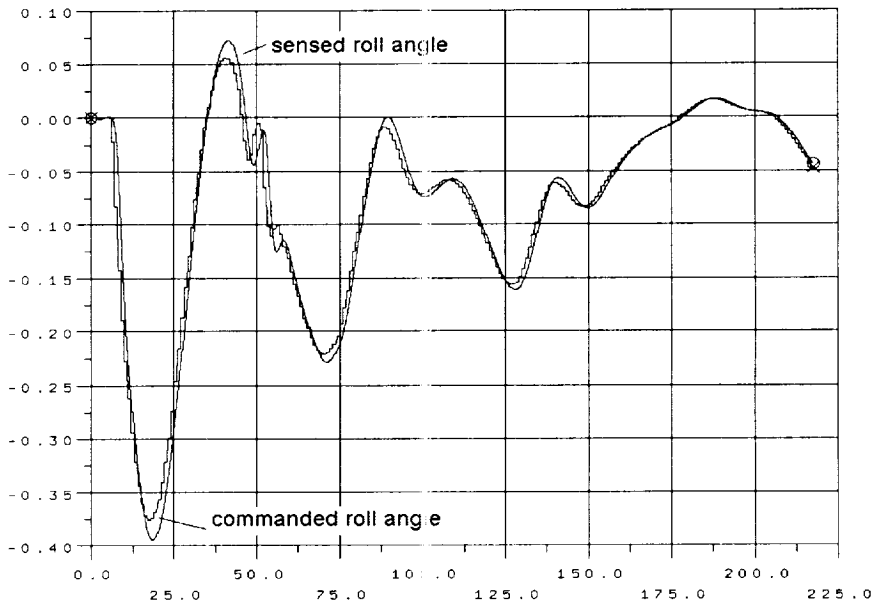

Fig. 1 Roll angle tracking (rad)

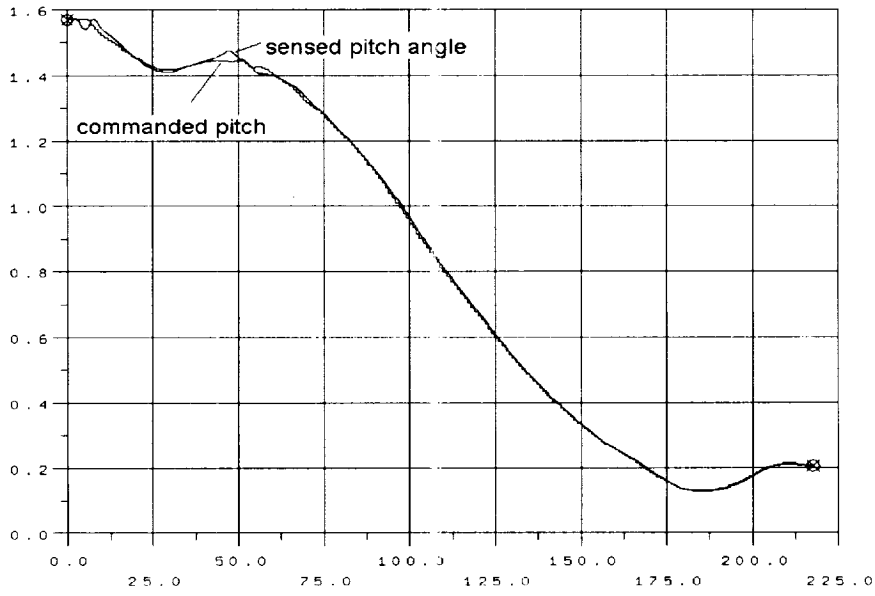

Fig. 2 Pitch angle tracking (rad)

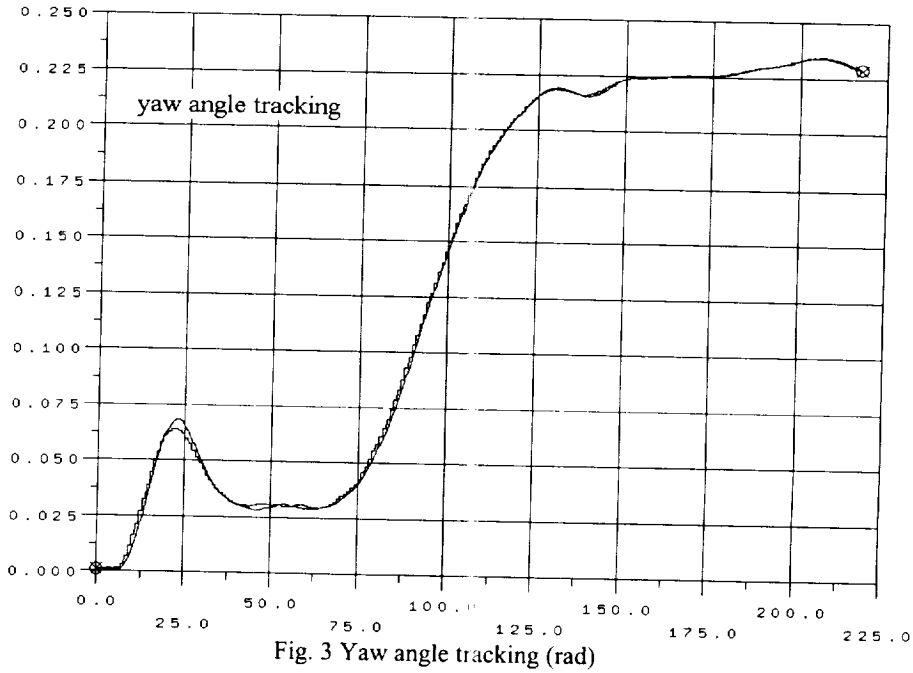

Fig. 3 Yaw angle tracking (rad)

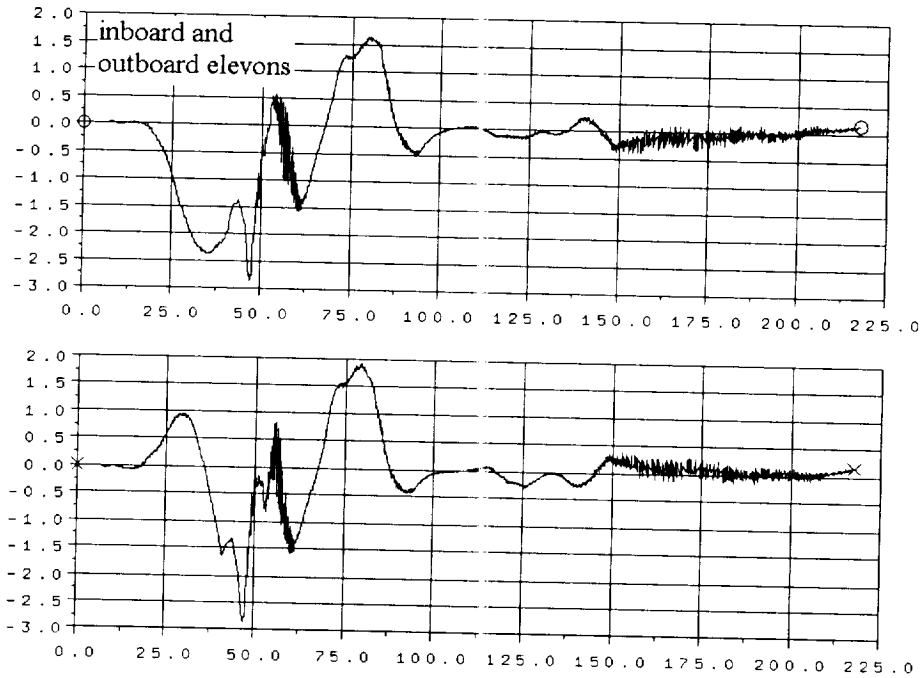

Fig. 4 Inboard and outboard elevon deflections (degrees)

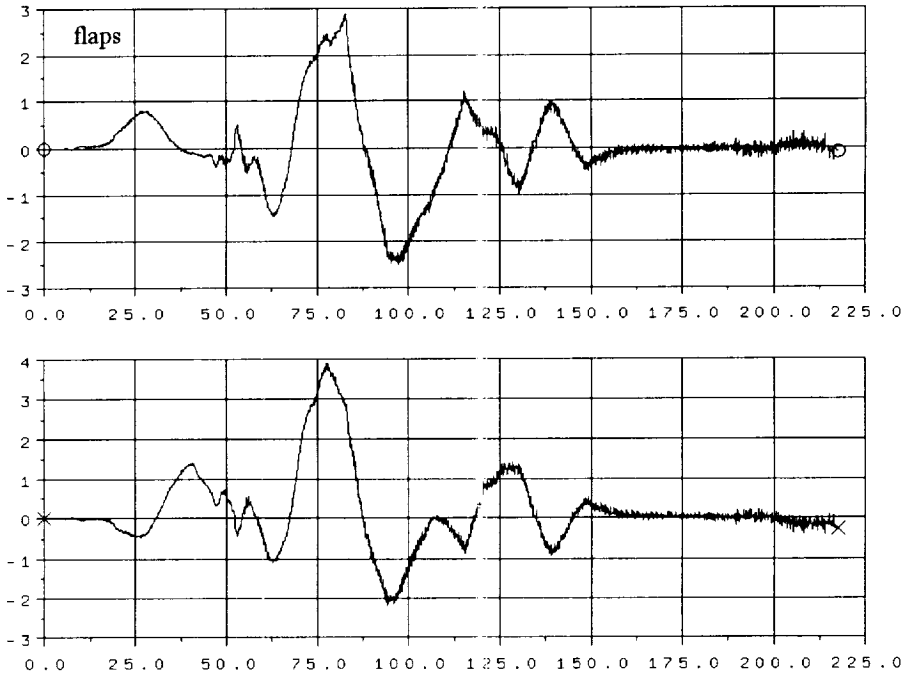

Fig. 5 Flap deflections (degrees)

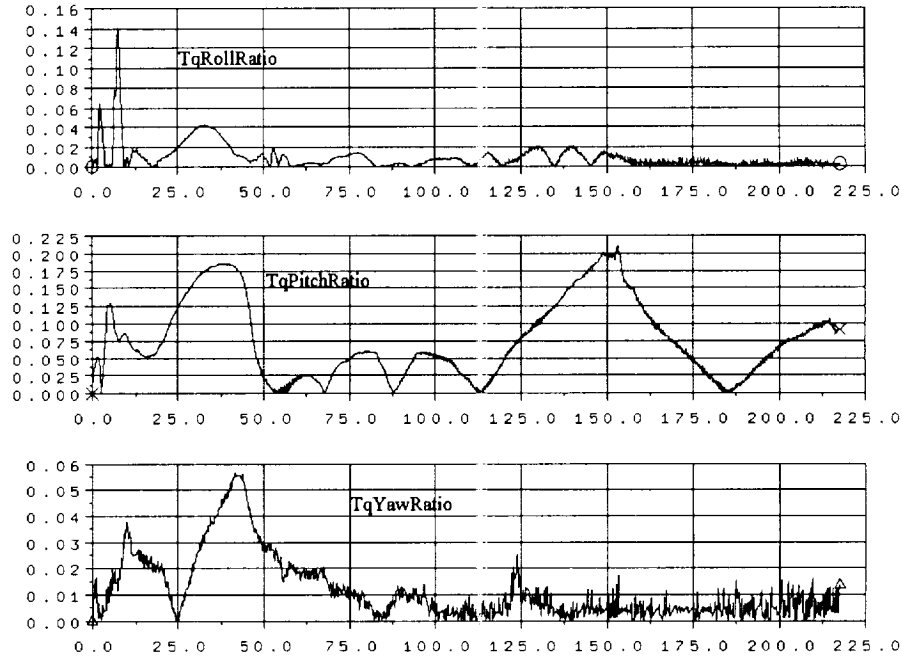

Fig. 6 Torque ratios

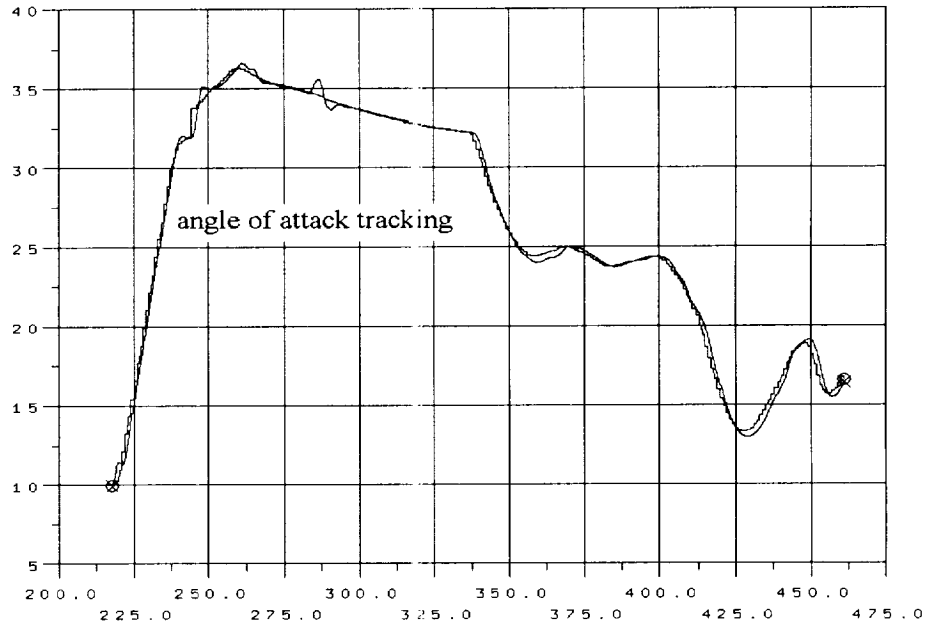

Fig. 7 Angle of attack tracking (degrees)

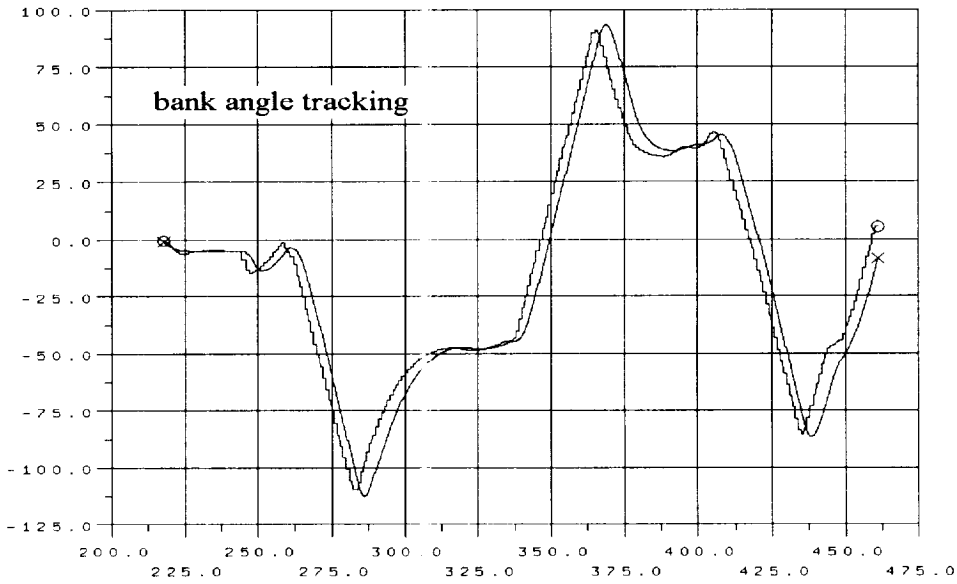

Fig. 8 Bank angle tracking (degrees)

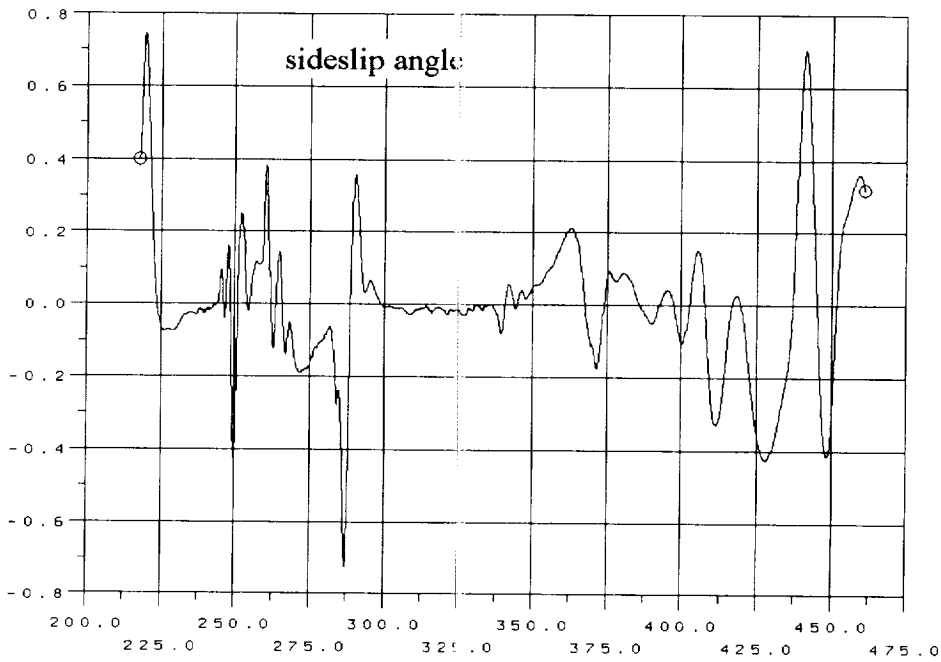

Fig. 9 Sideslip angle tracking (degrees)

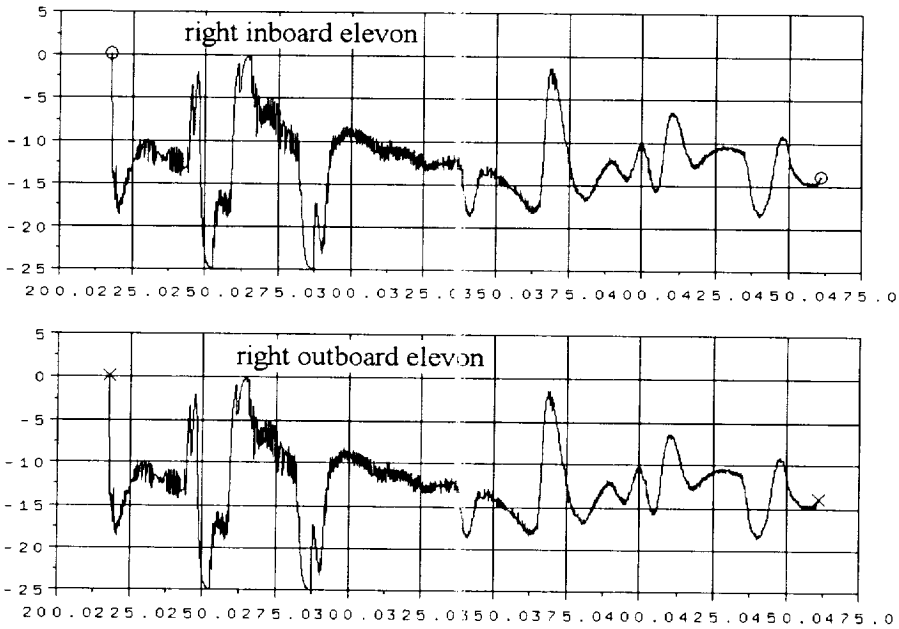

Fig. 10 Elevon deflections (degree)

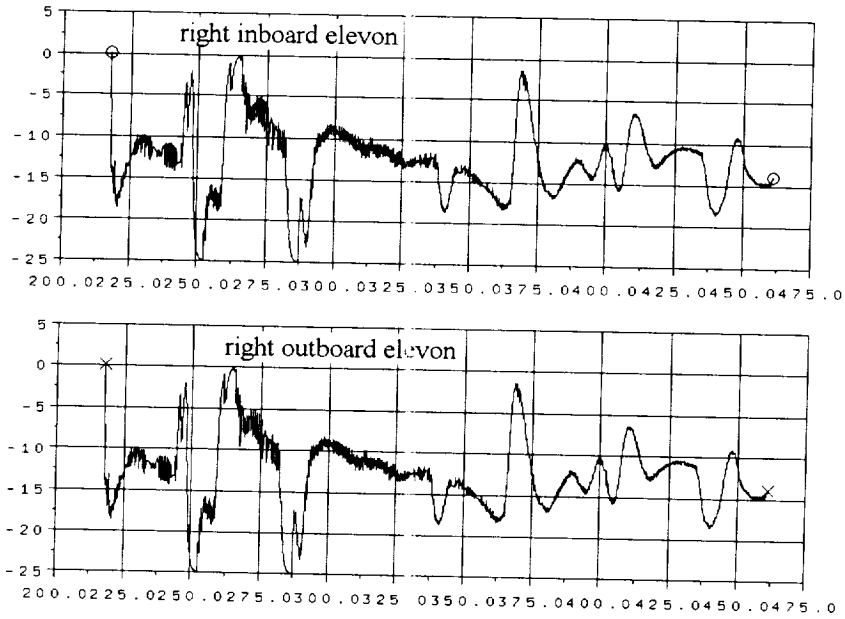

Fig. 11 Flap deflections (degrees)

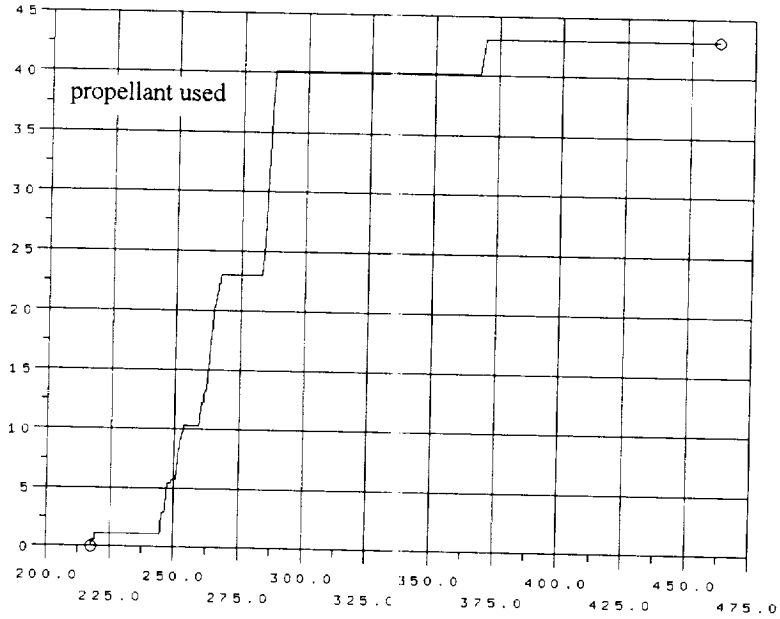

Fig. 12 RCS propellant used (lb)

Summary of the Test1 Results

- The nominal mission trajectory was successfully followed, with all trajectory parameters well within the limits.
- Control algorithm design depends only on mass property of RLV providing robustness that leads to risk and cost reduction.
- Reduced development costs is demonstrated by significant reduction of design/tuning parameters from 7500 in gain-scheduled PID controller to 36 in TV-SMC.
- Capability for cost reduction is demonstrated by saving 455 lb of the RCS propellant.

Test 2. Dispersion case evaluation.

The goals and implementation conditions of the dispersion case evaluation test areRobustness to RLV and environment dispersions are to be demonstrated in 75 dispersion runs using TV-SMC/adaptive gain algorithm.

- The aerodynamic model and actuator model is based on X-33 vehicle data

The results of dispersion runs are demonstrated for *descent* only. The bandwidth adaptation in the outer loop TV-SMC is shown in Figure 13. The angle of attack, bank angle and sideslip angle dispersion evolution is demonstrated in Figure 14. Angle of attack and bank angle tracking errors are depicted in Figure 15 and demonstrate a reasonable dispersion tracking accuracy. Elevon and flap dispersion deflections are shown in figures 16 and 17. They demonstrate acceptable performance. The RCS propellant used in *descent* is shown in Figure 18. The *ascent* dispersion runs are also successful.

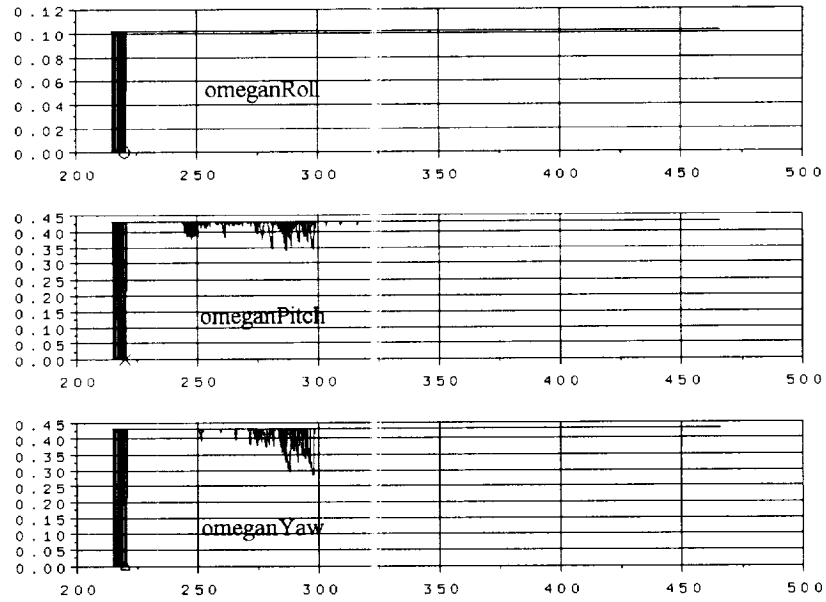

Fig. 13 Outer loop bandwidth adaptation

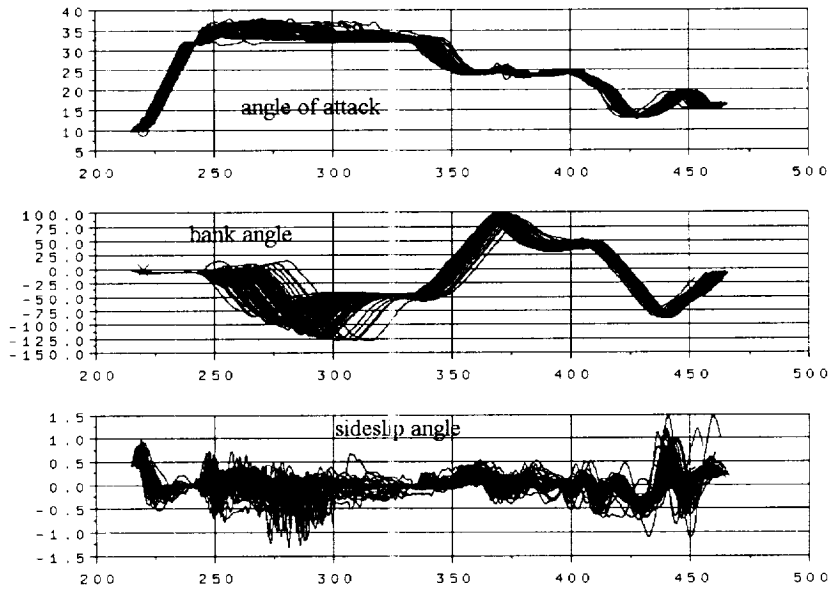

Fig. 14 Angle of attack, bank and sideslip angles (degrees)

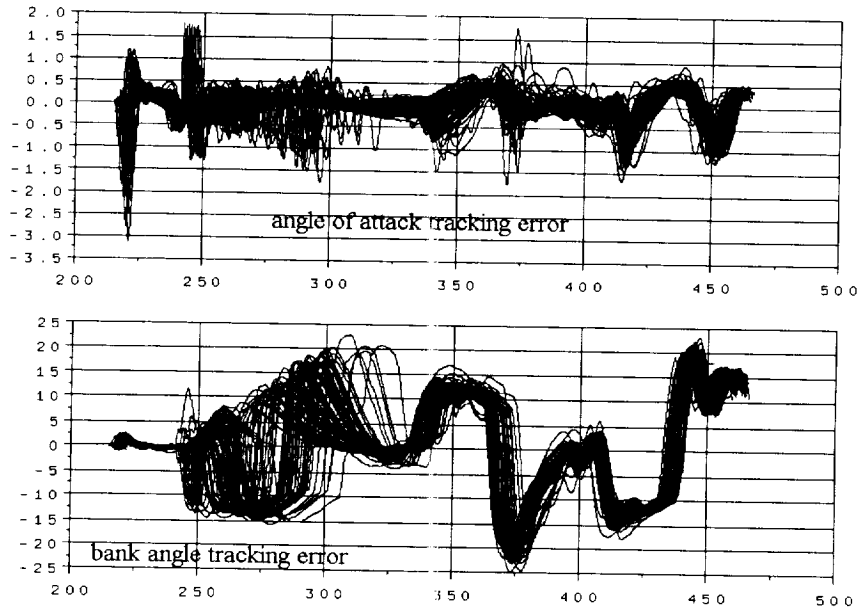

Fig. 15 Angle of attack and bank angle tracking errors (deg)

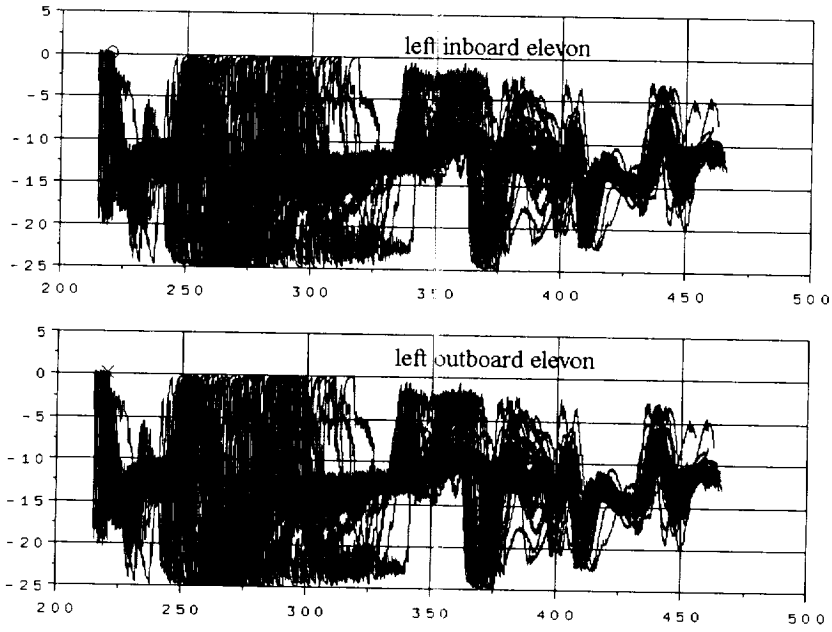

Fig. 16 Elevon deflections (degrees)

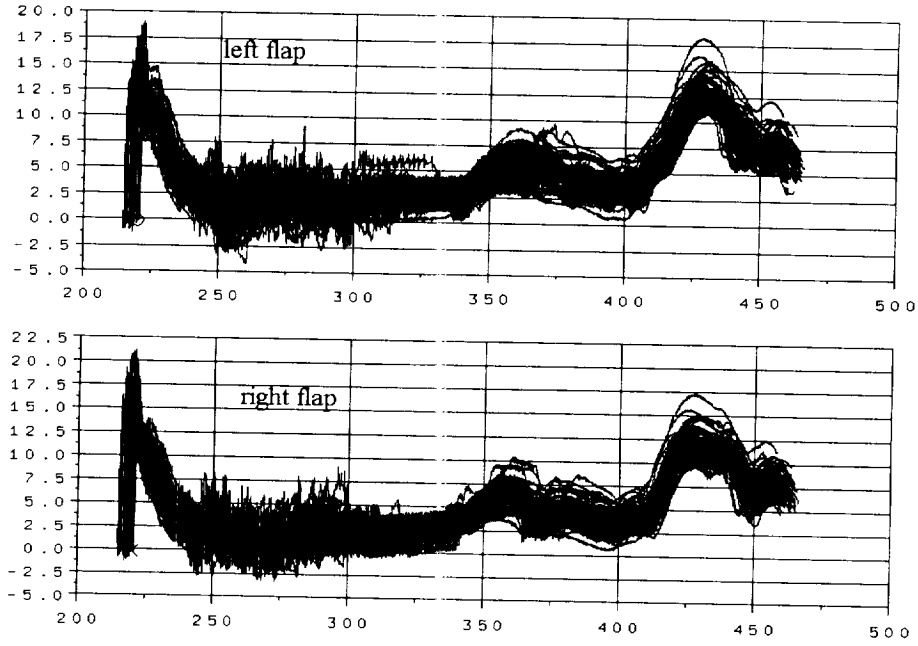

Fig. 17 Flap deflections (degrees)

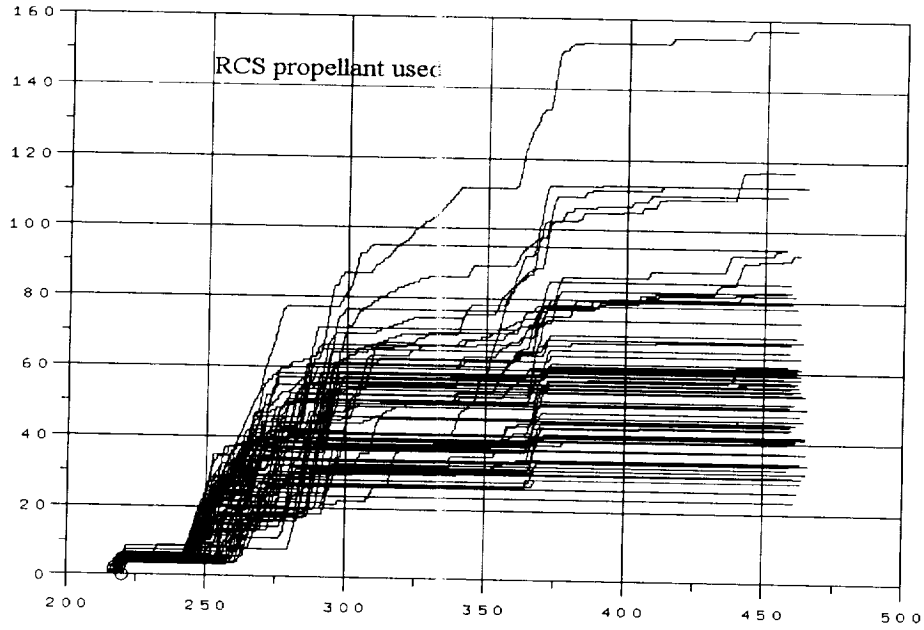

Fig. 18 RCS propellant used (lb)

*Summary of the Test2 Results*All 75 dispersion trajectories were successfully followed in ascent and descent, with all trajectory parameters well within the limits.

- Capabilities of significant saving of RCS propellant, 340 lb, which amounts to $340,000 saving if the weight is used for payload, is demonstrated.

Test 3. Actuator-failed flight evaluation.

The goals and implementation conditions of the actuator-failed *descent* flight evaluation test are

- Demonstrate capability for providing adaptation to non-catastrophic failures and increase mission success rate by means of changing bandwidths via TV-SMC.
- Control commands shall be adaptive to failures and degraded performance.
- The aerodynamic model and actuator model is based on X-33 vehicle data.

In Figure 19 inboard elevon deflections are demonstrated. It is clear that the left inboard elevon is in a hard on position (actuator failure). Time-varying TV-SMC outer loop gains demonstrate SMC gain adaptation in Figure 20. A corresponding angle of attack, bank angle and sideslip angle tracking is shown in Figures 21, 22 and 23. The plots demonstrate a high tracking accuracy in presence of actuator failure.

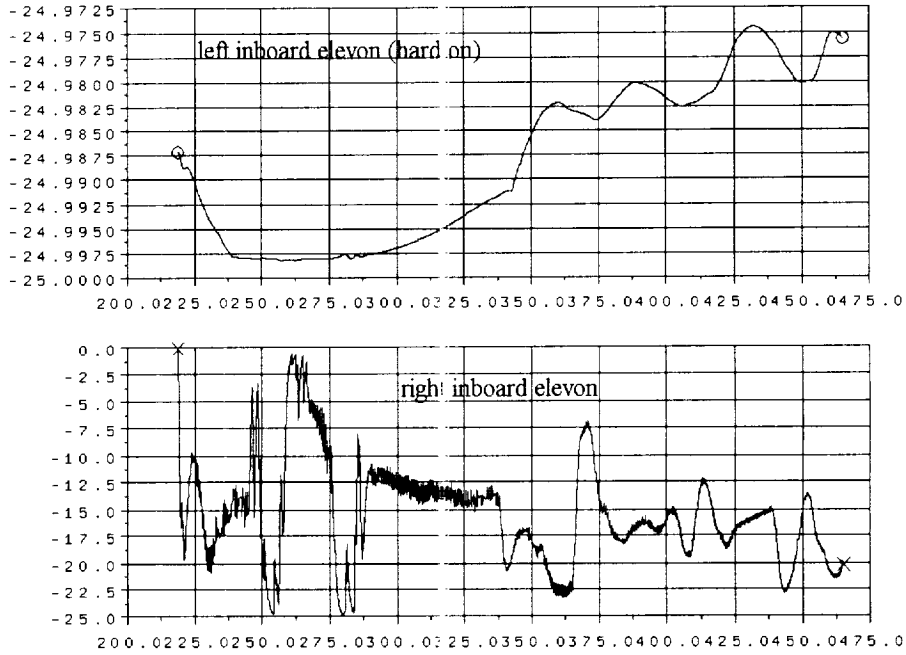

Fig. 19 Inboard elevon deflections

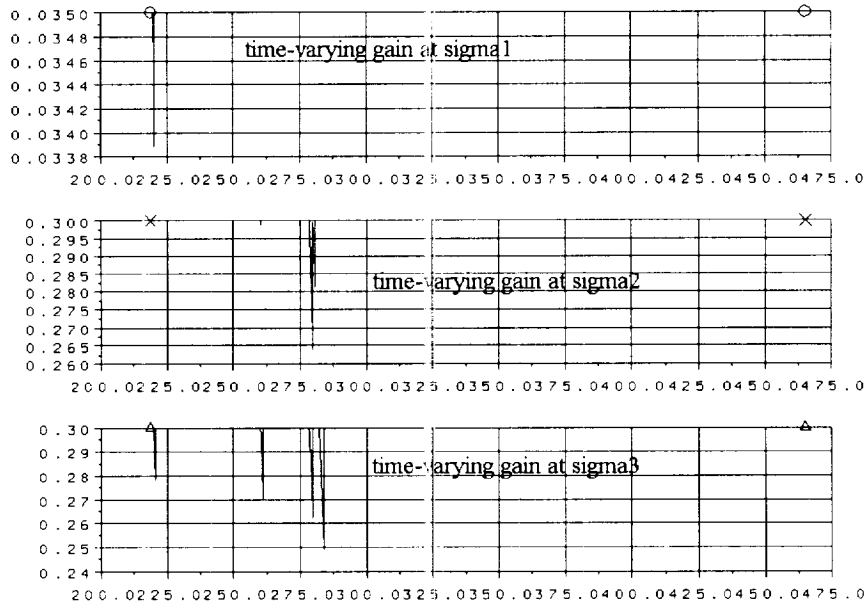

Fig. 20 TV-SMC gain adaptation

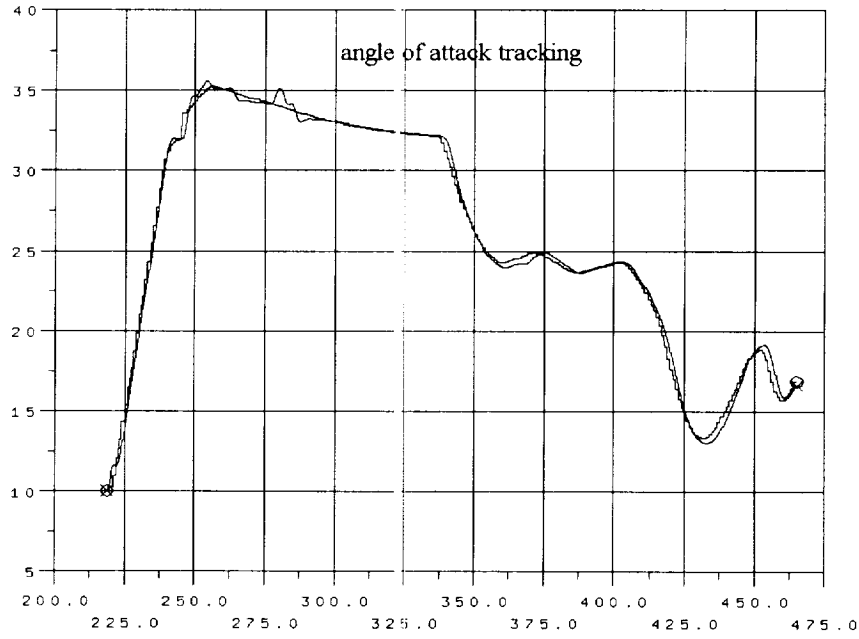

Fig. 21 Angle of attack tracking (degrees)/ failure case

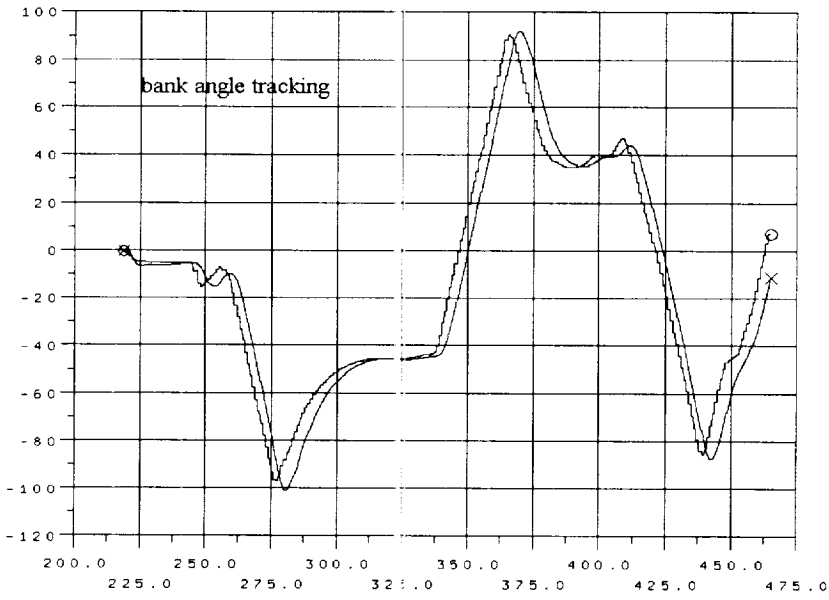

Fig. 22 Bank angle tracking (degrees)/ failure case

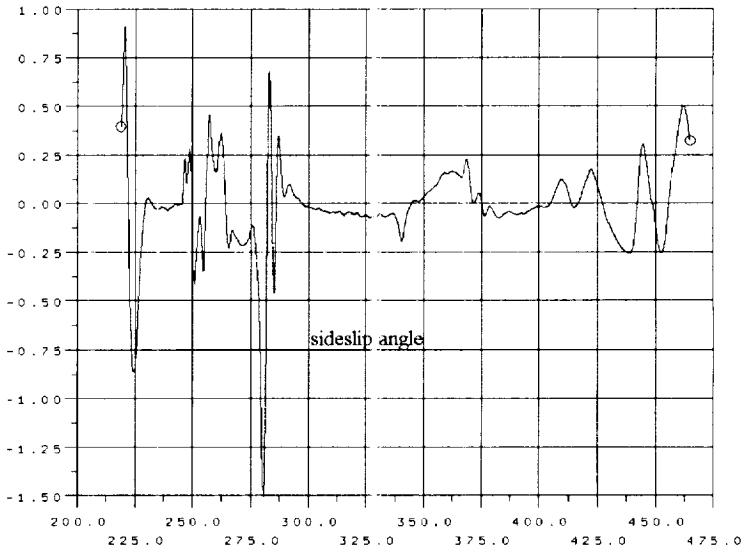

Fig. 23 Sideslip angle tracking (degrees)/ failure case

Summary of the Test3 Results

- The nominal trajectory was successfully followed in descent with the left inboard elevon in hard on position, with all trajectory parameters within the limits.
- Capability for providing adaptation to non-catastrophic failures and increase mission success rate by means of changing bandwidths via TV-SMC/adaptive gain algorithm is demonstrated.
- Control commands are adaptive to failures and degraded performance.

8. SUMMARY AND CONCLUSIONS

The time-varying sliding mode controller (TV-SMC) design algorithm is developed for the 2nd generation reusable launch vehicle in ascend and descend modes. In order to maintain stability, the bandwidth of the nominal (reduced-order) system is reduced accordingly using a time-varying bandwidth PD-eigenstructure assignment technique. The presented TV-SMC fault-tolerant technique automatically handles momentary saturations and integrator windup caused by excessive disturbances, guidance command or dispersions under normal vehicle conditions. The TV-SMC

algorithm has been coded and successfully simulated for the X-33 technology demonstration vehicle in ascent and descent modes using high fidelity 6DOF mathematical model.

9. REFERENCES

1. Hall, C. E., Hodel, A. S., and Hung, J. Y., "Variable Structure PID Control to Prevent Integral Windup", *Proceedings of the 31st Southeastern Symposium on System Theory*, IEEE, 1999, pp. 169-173.

2. DeCarlo, R. A., Zak, S. H., and Matthews, G. P. "Variable structure control of nonlinear multivariable systems: a tutorial," *IEEE Proceedings*, Vol. 76, 1988, pp. 212-232.

3. Utkin, V. I., *Sliding Modes in Control and Optimization*, Berlin, Springer - Verlag, 1992, pp. 15-82.

4. Hung, J. Y., Gao, W., and Hung, J. C., "Variable Structure Control: A Survey," *IEEE Transactions on Industrial Electronics,* Vol. 40, No. 1, 1993, pp. 2-21.

5. Shtessel, Y., Hall, C., and Jackson, M. ,"Reusable Launch Vehicle Control in Multiple Time Scale Sliding Modes," *AIAA Journal on Guidance, Control, and Dynamics,* Vol. 23, No. 6, pp. 1013-1020, 2000.

6. Shtessel, Yuri B. and Hall, Charles E., "Multiple time scale sliding mode control of reusable launch vehicles in ascent and descent modes," *Proceedings of American Control Conference*, Washington, DC, June 2001.

7. Zhu, J., Banker, B. D., and Hall, Charles E., "X-33 ascent flight controller design by trajectory linearization - a singular perturbational approach," AIAA-2000-4159, *AIAA Guidance, Navigation and Control Conference*, Denver, Colorado, Aug. 2000.

8. Zhu, J., Hodel, A. Scott, Funston, K., and Hall, C. E., "X-33 entry flight controller design by trajectory linearization - a singular perturbational approach," *Proceedings of American Astronautical Society Guidance and Control Conference,* pp. 151-170, Breckenridge, Colorado, Jan. 2001.

9. H. Khalil, *Nonlinear Systems,* Second Edition, Prentice Hall, 1996.